

Collective excitations and instabilities in multi-layer stacks of dipolar condensates

Daw-Wei Wang¹, and Eugene Demler²

¹Physics Department and National Center for Theoretical Science,
National Tsing Hua University., Hsinchu, Taiwan

²Physics Department, Harvard University, Cambridge, MA 02138, USA
(Dated: February 21, 2024)

We analyze theoretically the collective mode dispersion in multi-layer stacks of two dimensional dipolar condensates and find a strong enhancement of the roton instability. We discuss the interplay between the dynamical instability and roton softening for moving condensates. We use our results to analyze the decoherence rate of Bloch oscillations for systems in which the s-wave scattering length is tuned close to zero using Feshbach resonance. Our results are in qualitative agreement with recent experiments of Fattori et al. on ³⁹K atoms.

Recently quantum degenerate gases and Bose condensates with dipolar interactions attracted considerable attention both theoretically [1,2,3] and experimentally [4,5,6]. The long range character and anisotropy of dipolar interactions is expected to lead to a variety of exotic many-body ground states [1,2,7,8] and unusual collective excitations [3]. A recent addition to this class of systems are ultracold atoms in which the s-wave scattering length can be tuned to zero using Feshbach resonance and thus enhancing the role of dipolar interactions [4]. In particular, groups in Florence and Innsbruck used one-dimensional (1D) optical lattices to create multi-layer stacks of pancake condensates in the regime of small s-wave scattering length and experimentally studied Bloch oscillations (BO) [9,10]. In this paper we analyze theoretically collective excitations in dipolar superfluids in the presence of a 1D periodic potential (Fig. 1 (a)). Compared to the single layer case we find that the roton instability is strongly enhanced and occurs at a much shorter wavevector, which is determined primarily by the inter-layer distance. We also observe interesting interplay between roton softening and dynamical instability for moving condensates. This implies that both the dynamical and roton instabilities should play an important role in the dynamics of Bloch oscillations. We compare our results for the decoherence rate of BO to experimental results of Fattori et al. [9] and find qualitative agreement.

We consider a multi-layer stack of two-dimensional (2D) condensates loaded in a 1D optical lattice with the magnetic dipolar moments (\mathbf{d}) oriented either perpendicular or parallel to the layer planes, depending on the direction of the external magnetic field (see Fig. 1 (a)). We start our analysis with the assumption that layers are infinitely large, but will consider finite size effects when comparing with the experimental results for the decoherence rate of BO. We further assume that the 1D periodic potential (which we take to be in the z-direction) is sufficiently strong so only the lowest single particle subband (wavefunctions, $\psi_j(z)$, where $j = 1; 2; \dots; L$ is the layer index and L is the total number of layers) is occupied in each layer, and $\psi_j(z)$ can be well-approximated by Gaussian functions of width W [3]. Integrating out the confinement wavefunction in the z direction, we obtain

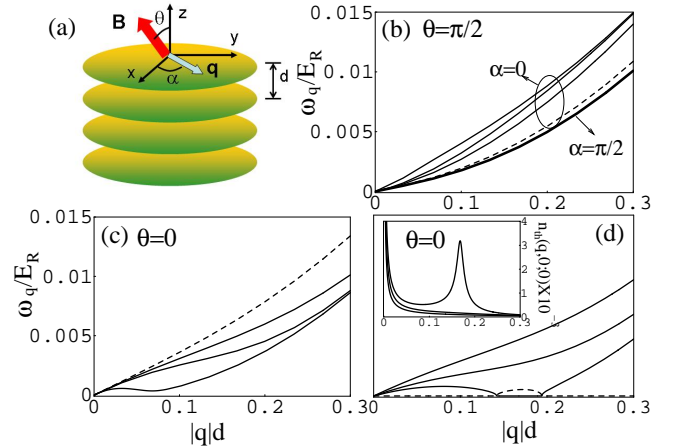


FIG. 1: (a) Dipolar condensate in a 1D optical lattice. External magnetic field, \mathbf{B} , is in the $x-z$ plane with an angle θ with respect to the lattice direction (z). α is the angle between the in-plane momentum \mathbf{q} of excitations and the x -axis. Figures (b) and (c) show collective mode dispersions for magnetic fields parallel and perpendicular to the layers respectively. The dashed curves are the single layer results for $\alpha = 0$, and the solid curves are for $L = 10, 20$, and 100 respectively from bottom to top in (b) and from top to bottom in (c). The three thin solid lines in (b) are results for $\alpha = 0$, while the thick solid line is for $\alpha = \pi/2$ and independent of L . Here we choose $a_s = 0.15a_0$. (d) Same as (c) but with $L = 10$ and different values of a_s : $a_s = 0.19, -0.38$, and $0.472a_0$ from top to bottom. The dashed line is the imaginary part of collective mode for $a_s = 0.472a_0$. Inset: Momentum distribution of thermal quasi-particles of the same system for $a_s = 0.19, -0.38$ and $-0.47a_0$ from bottom to top with $T = 100$ nK.

the intra-layer interaction:

$$V_0(\mathbf{q}) = \frac{g_s + 2P_2(\cos\theta)g_d}{W} \frac{P_2(\cos\theta)}{2} \quad (1)$$

where $g_s = \frac{4\pi\hbar^2 a_s}{m}$ and $g_d = \frac{0.4}{3} \frac{\hbar^2}{m} \frac{1}{\cos^2\theta \cos^2\alpha - \sin^2\theta}$ with a_s and m being the s-wave scattering length and the atom mass. $P_2(\cos\theta) = \frac{3}{2} \cos^2\theta - \frac{1}{2}$ with θ being the angle between dipole moment and the z -axis (direction of optical lattice) and α being the angle between in-plane

momentum q and the x -axis, which is set to be the dipole moment direction when the magnetic field is parallel to the layer (see Fig. 1(a)). Finally, $P_2(x) = \frac{1}{2}(3x^2 - 1)$ is the Legendre polynomial and $F(q) = \frac{1}{2}W \frac{q}{q+1} \text{Erf}\left(\frac{q}{2}\right) e^{q^2 W^2/2}$ with $\text{Erf}(x)$ being the Error function. Similarly, the inter-layer interaction matrix element between layers j and j^0 ($1 \leq j, j^0 \leq L$) can be also calculated:

$$V_1(q) = \frac{3g_d e^{-\frac{1}{2}d^2 = 2W^2 \cos^2}}{W \frac{q}{q+1}} \frac{3g_d}{2} \left(\frac{dk_z}{2} \frac{\cos(ldk_z) e^{-\frac{1}{2}k_z^2 W^2}}{1 + k_z^2 = q^2} \right) : (2)$$

We note that for the case of perpendicular field ($\theta = 0$), $V_1(q) = \frac{3g_d}{2} e^{-\frac{1}{2}d^2} e^{-\frac{1}{2}k_z^2 W^2}$ as $W \rightarrow \infty$, showing a strong attraction at a characteristic length scale, ld . As we discuss below, such feature will lead to the wavevector of roton excitations being much smaller than the corresponding wavevector in a single layer system [3].

Our starting point is the microscopic Hamiltonian: $H = \sum_{q,k} 2J(1 - \cos(kd)) + \sum_q \left(b_{q,k}^\dagger b_{q,k} + \frac{1}{2L} \sum_k \left(\frac{dq}{(2)^2} \right) \hat{a}_k(q) \hat{a}_k(q) \right) \mathcal{M}_k(q)$, where $\frac{1}{2L} \sum_k \left(\frac{dq}{(2)^2} \right) \hat{a}_k(q) \hat{a}_k(q) \mathcal{M}_k(q)$ is the bosonic field operator for magnetic atoms, and $\mathcal{M}_k(q) = \sum_{p,j,k^0} b_{p+q,j,k^0}^\dagger b_{p,j,k^0}$ is the density operator. $\nabla(q;k) = \sum_{j=1}^L V_j(q) e^{-ikjd}$. The chemical potential is determined from the condition that collective modes are gapless in the long wavelength limit. The summation on k is within the first Brillouin zone, $-\pi/d < k < \pi/d$.

When discussing collective excitations we consider a general case of dipolar condensate moving in the z -direction. Assuming that the moving condensate has a macroscopic number of particles in a state with lattice momentum k_0 , the dispersion of Bogoliubov modes in the co-moving frame is given by

$$\epsilon(q;k;k_0) = \sum_h \left(E_{k_0}^0(k) + \epsilon^0(q) \right) \pm \sqrt{E_{k_0}^0(k) + \epsilon^0(q) + 2n_0 \nabla(q;k)} ; (3)$$

Here $E_{k_0}^0(k) = 2J \cos(k_0 d) (1 - \cos(kd))$, n_0 is the 2D condensate density in each layer, k and q are the z - and in-plane components of the excitation momentum. Instabilities manifest themselves as imaginary frequencies in Eq. (3). There are three distinct mechanisms of instabilities: (i) when $k_0 d > \pi/2$ and $\nabla(0;0) > 0$ we find the usual dynamical instability [11,12], which can be understood as coming from the negative effective mass caused by the lattice band structure; (ii) when $\nabla(0;0) < 0$ we have a 3D collapse of the condensate [4]; (iii) instability at a finite momentum q due to the softening of roton excitations. The latter is a unique feature of long-ranged dipolar interactions in low-dimensional systems [3]. In the rest of this paper, we will analyze distinct roles played by these three instabilities in the dynamical properties of moving condensates. For numerical calculation, we take

system parameters similar to Florence's group [9] on ^{39}K , where the distance between the layers is $d = 0.516$ nm and the strength of the optical potential is $V_0 = 6E_R$ (here $E_R = 4.8$ k Hz is the recoil energy). As a result, $J = 0.0645E_R$, and the Gaussian width of each layer is $W = 0.203d$. Throughout this paper, we will use $L = 10$ and $n_0 = 10^{10} \text{ cm}^{-2}$, unless specified differently.

To demonstrate the importance of inter-layer coupling, in Fig. 1(b) and (c) we show the calculated in-plane collective mode dispersion of a static ($k_0 = 0$) condensate for different numbers of layers, L (we set the z -component of the excitation momentum to zero, $k_z = 0$). We analyze cases of the magnetic field (dipole moments) being either perpendicular ($\theta = 0$) or parallel ($\theta = \pi/2$) to the planes of the condensate pancakes. For the perpendicular field case (Fig. 1(c)), the long wavelength behavior of the collective mode changes dramatically as the number of layers in the stack increases. Roton excitation becomes softened at a small but finite in-plane momentum. By contrast, when the magnetic field is parallel to the pancakes and q is along the field (i.e. $\theta = \pi/2$ and $\theta = 0$, Fig. 1(b)), the energy of excitations is real and goes up with the increase of the number of layers. Dependence on the number of layers is not present for in-plane magnetic field but q being perpendicular to the direction of the field, since $\theta = \pi/2$ or $\theta = 0$ in Eq. (2). These features can be understood using the following simple argument. Dipolar interaction is attractive when dipoles are oriented head-to-tail and repulsive when they are oriented side-by-side. So for perpendicular magnetic field increasing the number of layers increases the attractive inter-layer component of the interactions but does not affect the repulsive intra-layer part. Conversely for the field parallel to the plane of the pancakes, increasing the number of layers primarily increases the repulsive part of the interactions. In Fig. 1(d), we show the collective mode dispersion for various values of a_s with ten layers, showing a roton softening when $a_s < 0.471a_0$ (a_0 is Bohr radius). One possible method of observing roton softening in experiments is to use time-of-flight experiments to measure the occupation of the in-plane momentum states. When a_s is close to the critical value of roton softening, the thermally excited quasi-particles begin to occupy the roton minimum and an incoherent peak at roton wavevector emerges. After releasing atoms from the trap, atoms propagate essentially as free particles thus quasi-particles at roton wavevector expand in the in-plane direction much faster than the condensate particles. As a result, for a sufficiently long expansion time, these particles should form a ring structure in the x - y plane. In the insert of Fig. 1(d) we show thermal particle occupation number, $n_{th}(q;k) = [\exp(\epsilon(q;k;0)/k_B T) - 1]^{-1}$, for $L = 10$ but different s -wave scattering length.

We now proceed to discuss the structure of unstable modes as a function of their momentum q for different values of the condensate momentum (k_0). Typical results for the perpendicular magnetic field are shown in Fig. 2. Several interesting features should be noted: (1)

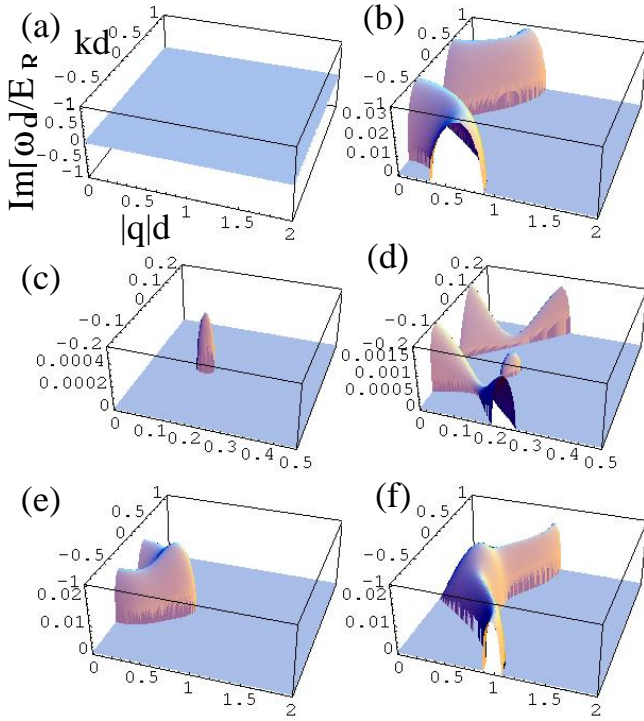


FIG. 2: Imaginary part of the collective mode as a function of $|q|d$ and kd for magnetic field perpendicular to the layer plane. The upper, middle, and lower panels are for $a_s = 1.88a_0$, $0.48a_0$, and $-1.88a_0$ respectively. $k_0d = 0.4$, and 0.6 respectively for the left and right columns. All other parameters are the same as in Fig. 1(d).

When the s-wave scattering length is positive, there is no instability for $k_0d < \sqrt{2}$ (see (a)). Dynamical instability occurs when $k_0d > \sqrt{2}$ (see (b)). (2) When the s-wave scattering length is negative but small, there is an instability due to the roton softening for $k_0d < \sqrt{2}$ (see (c)). (3) When the s-wave scattering length is negative and large, there is another instability channel coming from the usual 3D collapse (see (e)). (4) Finally, the complicated interplay between the dynamical instability, roton-softening, and the collapse takes place for $k_0d > \sqrt{2}$, as can be observed in (d) and (f). Such abundant structure of unstable modes is unique to dipolar condensates in multi-layer systems. We note that earlier theoretical studies of the dynamical instability [12] did not consider the in-plane character of excitations. Hence all the earlier analysis was performed for systems which were effectively one dimensional. Our results indicate that the in-plane structure of collective modes is crucial when analyzing system with dipolar interactions.

In Ref. [9], the decoherence rate of BO was defined based on the growth rate of the momentum distribution of atoms in the z -direction. Our next step is to connect our analysis of instabilities of states with a fixed momentum k_z to the dynamics of BO. This can be done using following reasonable approximations: (1) In the process of BO, k_0 undergoes periodic oscillations

and covers the entire Brillouin zone. Since the number of non-condensate particles grows exponentially with a rate proportional to the imaginary part of the collective mode [13], we can calculate the growth rate of the momentum distribution $(\langle q; k \rangle)$ in a BO by averaging $\text{Im}[\langle q; k; k_0 \rangle]$ over all possible values of k_0 : i.e., $\langle q; k \rangle = \frac{1}{2} \int_0^{2\pi} dk_0 \text{Im}[\langle q; k; k_0 \rangle]$. (2) In the experiment, condensates are prepared at a fixed positive value of the scattering length (a_{in}) before the magnetic field is changed abruptly to a different value for studying BO [14]. In our calculation, we use Bose-Einstein distribution for the initial non-condensed particle distribution, i.e. $n_{\text{in}}(q; k) = n_{\text{th}}(q; k)$ with $a_{\text{in}} = 3a_0$ [9] and $T = 100$ nK. (3) To include the effect of in-plane confinement, we introduce an infrared in-plane momentum cut-off, q_c , which should be of the order of the inverse of the system size. In other words, we assume that excitations with $|q| < q_c$ are not relevant. (4) Finally, to simplify calculations, we assume that the condensate density is the same in all layers. We believe that these approximations correctly capture the phenomena taking place in experiments reported in Refs. [9]. They also provide a general framework for understanding the role of interactions in BO experiments with dipolar condensates.

The time dependence of the width of the momentum distribution can now be calculated: $K_z(t) = \frac{1}{N_{\text{in}}} \frac{1}{L} \int_{-L/2}^{L/2} dk \int_{-L/2}^{L/2} \frac{dq}{(2\pi)^2} n_{\text{in}}(q; k) k^2 e^{i(q; k)t}$, where $\int_{-L/2}^{L/2} dk$ is the integral of all the in-plane momentum with $|q| > q_c$. $N_{\text{in}} = \frac{1}{L} \int_{-L/2}^{L/2} dk \int_{-L/2}^{L/2} \frac{dq}{(2\pi)^2} n_{\text{in}}(q; k)$ is the total number of initial non-condensate atoms. In the limit of small time, $K_z(t) = K_z(0) (1 + t + \dots)$ with

$$\frac{1}{K_z(0)^2} \frac{1}{L} \int_{-L/2}^{L/2} dk \int_{-L/2}^{L/2} \frac{dq}{(2\pi)^2} n_{\text{in}}(q; k) k^2 \langle q; k \rangle \quad (4)$$

being the growth rate of the cloud size in z direction (i.e. the decoherence rate defined in Ref. [9]). Eq. (4) establishes a connection between instabilities of collective modes and the decoherence rate of BO.

In Fig. 3, we show the calculated $K_z(t)$ as a function of a_s , for ten layers of ^{39}K atoms. Here we use $q_c = 1/33d = 2\pi/R_k$, where $R_k = 2.42 \mu\text{m}$ is the oscillator length (i.e. approximate system size for small a_s) of the in-plane trapping potential with trapping frequency 44 Hz [9]. We point out several important features: (1) for the magnetic field perpendicular (parallel) to the layer plane, K_z has a minimum at $a_s = 0.5a_0$ ($+0.38a_0$). These are different from zero due to dipolar interaction effects as originally suggested in Ref. [9]. (2) The minimum we obtained can be considerably smaller than 1 Hz. This suggests that the maximum coherence time observed in experiments may be limited by other mechanisms, such as inhomogeneous density between different layers or laser stability [9]. Such additional effects not included in our analysis may also explain why our calculated positions of minimum decoherence rate are of the same order but still different from the experimental results [9]. (3) We

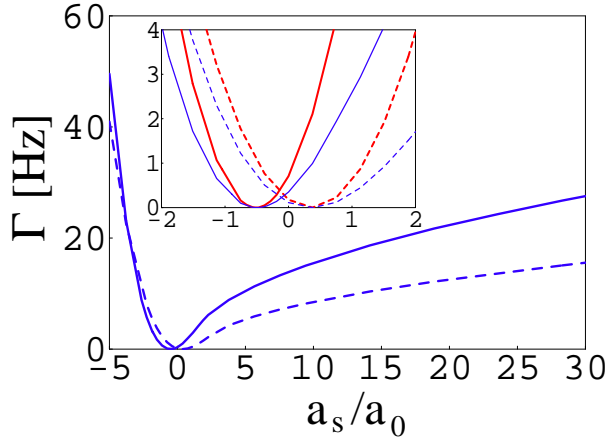


FIG. 3: Decoherence rate of a condensate BO as a function of a_s . The solid (dashed) line is for $q_d = 0$ ($q_d = 2$). $q_d = 1.33$ and other parameters are the same as used in Fig. 1(d). Inset: Magnified results near the minimum value. The red (or higher) curves are results using $q_d = 0.8$ for comparison.

emphasize, however, that the qualitative features of the decoherence rate are in good agreement with experiments in a wide range of scattering length. For example, the decoherence rate is not symmetric for the positive and negative scattering length regime when away from the position of minimum. This is not surprising since in the former case the decoherence is dominated by the dynamical instability (for $|k_0| > \pi/2$) whereas for the latter case it comes from the global collapse (for $|k_0| < \pi/2$). Furthermore, the dependence of the decoherence rate on the scattering length has a positive curvature near the minimum, and a negative curvature for larger positive values of a_s . The magnitude of Γ in the large a_s regime is of the order of tens of Hz, also in agreement with the experimental results of Ref. [9]. (4) Finally, we find that the decoherence rate is highly dependent on the initial momentum distribution, system size, and other system parameters. For example, in the inset we also present results calculated with a smaller infrared cutoff ($q_d = 0.8$), i.e. a larger in-plane system size. We observe a considerable increase in the value of decoherence rate (red lines),

indicating the important contribution from the instability in the long-wavelength limit. Detailed analysis (not presented here) also indicates that the decoherence rate can be very sensitive to the initial system temperature as well as the 2D density of atoms within individual pancakes. All of these effects originate from the in-plane instabilities in the stack of multi-layer dipolar condensate, which were not included in earlier theoretical analysis. Therefore, our model provides an alternative mechanism for explaining the decoherence rate of BO oscillations in experiments by Fattori et al. [9]. We point out that our analysis provides a fundamental limit on the decoherence rate of Bloch oscillations which arises from dipolar interactions for ultracold atoms and molecules.

Before concluding this paper we would like to mention that our results imply greater stability of supersolid phases in multi-layer systems. It was argued before that roton softening can lead to supersolid phases which correspond to macroscopic occupation both at zero and roton softening wavevector. In the case of a single layer system, roton softening occurs at short wavelengths (order of layer width), and therefore is expected to lead to a global collapse after exciting higher transverse modes. In a multi-layer system we consider here, the roton softening occurs at wavelengths much larger than the layer width. This strongly suggests that supersolid phases should be considerably more stable in multi-layer systems.

In conclusion we analyzed theoretically collective excitations in a multi-layer stack of two dimensional dipolar condensates. We found strong enhancement of roton softening and discussed its interplay with the dynamical instability. We showed important consequences of mode softening for the decoherence rate of Bloch oscillations. Our results are in qualitative agreement with experiments in Ref. [9]. We also make several concrete predictions for future experiments.

We acknowledge stimulating discussions with M. Fattori, G. M. Modugno, M. Inguscio, G. Shlyapnikov, and T. Pfau. This work was supported by the NSF grant DMR-0705472, Harvard-MIT CUA, DARPA, MURI, and NSC in Taiwan.

- ¹ M. Baranov, et al, Phys. Scripta T 102, 74 (2002); B. Deeb and L. You, Phys. Rev. A, 64, 022717 (2001); S. Yi and L. You, Phys. Rev. A, 61, 041604(R) (2000).
- ² G. Pupillo, et al, Phys. Rev. Lett. 100, 050402 (2008); H. P. Buchler, et al, Phys. Rev. Lett. 98, 060404 (2007); A. Micheli, et al, Phys. Rev. A 76, 043604 (2007).
- ³ S. Ronen, et al, Phys. Rev. Lett. 98, 030406 (2007); R. M. Wilson, et al, Phys. Rev. Lett. 100, 245302 (2008); U. Weiser, et al, Phys. Rev. A 73, 031602(R) (2006).
- ⁴ J. Stuhler, et al, Phys. Rev. Lett. 95, 150406 (2005); T. Lahaye, et al, Nature 448, 672 (2007).
- ⁵ S. Giovanazzi, L. Santos, and T. Pfau, Phys. Rev. A 75,

- 015604 (2007).
- ⁶ M. Vengalattore, et al, Phys. Rev. Lett. 100, 170403 (2008).
- ⁷ D.-W. Wang, et al, Phys. Rev. Lett. 97, 180413 (2006); D.-W. Wang, Phys. Rev. Lett. 98, 060403 (2007).
- ⁸ A. Arguëlles and L. Santos, Phys. Rev. A 75, 053613 (2007); C. Kollath, et al, Phys. Rev. Lett. 100, 130403 (2008); C. Chang, et al, arXiv:0807.1166 (unpublished).
- ⁹ M. Fattori, et al, Phys. Rev. Lett. 100, 080405 (2008); *ibid.* 101, 190405 (2008).
- ¹⁰ M. Gustavsson, et al, Phys. Rev. Lett. 100, 080404 (2008).
- ¹¹ M. Krammer, et al, Phys. Rev. Lett. 88, 180404 (2002); F. S.

- Cataliotti, et al, New J.Phys. 5, 71 (2003);
- ¹² B.Wu and Q.Niu, Phys. Rev. a 64, 061603(R) (2001);
A.Smerzi, et al, Phys. Rev. Lett. 89 170402 (2002); C.Menotti, A.Smerzi, and a.Trombettoni, New J.Phys. 5, 112 (2003); A.Polkovnikov and D.W.Wang, Phys. Rev. Lett. 93, 070401 (2004).
- ¹³ L.Fallani, et al, Phys.Rev.Lett. 93, 140406 (2004).
- ¹⁴ We note that they did not prepare the system in this method for the BO in the large and positive value of a_s . Here, for simplicity, we assume the initial distribution (a_{in} and q_c) are the same for BOs in all values of a_s .